The Open Dentistry Journal
DOI: 10.2174/0118742106389355250611102139, 2025, 19, e18742106389355
ISSN: 1874-2106

SYSTEMATIC REVIEW **OPEN ACCESS**

Volumetric Measurement of Alveolar Clefts for Bone Graft Planning: A Systematic Review

Inka Saraswati[1,*], Menik Priaminiarti[1], Norifumi Nakamura[2,3], Bramma Kiswanjaya[1], Dwi Ariawan[2] and Heru Suhartanto[4]

[1]*Department of Dentomaxillofacial Radiology, Faculty of Dentistry, University of Indonesia, Salemba Raya No.4, Central Jakarta 10430, Indonesia*
[2]*Department of Oral and Maxillofacial Surgery, Faculty of Dentistry, University of Indonesia, Salemba Raya No.4, Central Jakarta 10430, Indonesia*
[3]*Department of Oral and Maxillofacial Surgery, Kagoshima University Graduate School of Dental and Medical Sciences, 8-35-1, Sakuragaoka, Kagoshima 890-8544, Japan*
[4]*Faculty of Computer Science, University of Indonesia, Jl. Lingkar Pondok Cina, Depok 16424, Indonesia*

Abstract:

Introduction: To investigate protocols for volumetric measurement of alveolar defect in alveolar cleft cases, including innovations in Artificial Intelligence (AI).

Methods: Searches were conducted using PubMed, Embase, and Scopus databases, along with a hand search. Based on inclusion and exclusion criteria, 17 studies were selected. Additionally, discussions on the protocols included workflow and anatomical landmarks associated with the measurement.

Results: Thirty workflows were identified and categorized into virtual and 3D printing-based approaches. A 3D U-Net architecture was employed for segmentation and measurement using artificial intelligence. Various anatomical landmarks for defining alveolar cleft boundaries were described. The average volume of the alveolar cleft was 1.61 cm^3.

Discussion: The majority of the studies were published within 3 years of the article search, indicating an increased desire to optimize the utilization of 3D imaging beyond simple assessments. Recent developments in AI have simplified complex imaging tasks; hence, volumetric assessments are expected to increase in the future.

Conclusion: The expert workflow with the most supporting evidence is manual tracing on the axial slice. Studies using AI are emerging and need to be explored. The anatomical landmarks advocated by this review are cementoenamel junction, anterior nasal spine, and continuity with the alveolar segments with adequate labio-palatal thickness as superior, inferior, and labio-palatal borders, respectively. Nonetheless, more studies are needed to help create a technical guideline.

Keywords: 3D imaging, Computed tomography (CT), Cone beam CT, Cleft lip and alveolus, Cleft palate, Volumetric measurement.

*Address correspondence to this author at the Department of Dentomaxillofacial Radiology, Faculty of Dentistry, University of Indonesia, Salemba Raya No.4, Central Jakarta 10430, Indonesia; Tel: +628121039826;
E-mail: inkasaraswati@office.ui.ac.id

Cite as: Saraswati I, Priaminiarti M, Nakamura N, Kiswanjaya B, Ariawan D, Suhartanto H. Volumetric Measurement of Alveolar Clefts for Bone Graft Planning: A Systematic Review. Open Dent J, 2025; 19: e18742106389355.
http://dx.doi.org/10.2174/0118742106389355250611102139

Received: February 03, 2025
Revised: April 07, 2025
Accepted: May 02, 2025
Published: June 13, 2025

1. INTRODUCTION

Cleft lip, alveolus, and/or palate are the most common craniofacial abnormalities [1]. Oral clefts occur in 0.3–0.45 per 1,000 births globally [2], and about 75% of cleft cases involve the alveolar bone and primary palate [3]. In those cases, Alveolar Bone Graft (ABG) surgery is recommended to ensure the eruption of lateral incisors and canines, maintain periodontal health of adjacent teeth, support orthodontic movement, provide a foundation for dental implants, reinforce the base of the nose, and close oronasal fistula [1]. However, both overfilling and underfilling of alveolar bone grafts have been reported, which lead to reduced success [4, 5]. Although there are several other factors that may influence the success of alveolar bone graft surgery, such as cleft type, eruption stage of canines, presence of fistulae, age, and preoperative orthodontics [3, 6, 7], any mismatch in the bone filling can be prevented by preoperatively determining the volume of graft needed. The clinical advantages of volumetric measurement in alveolar bone graft surgical planning, especially with iliac ridge donors, are discussed in the study conducted by Virani *et al*. [8]. Additionally, some institutions use donor sites with more limited bone resources, such as chin bone. In these cases, volumetric assessment informs surgeons about the amount of bone required, whether the selected donor site can provide sufficient volume, and whether additional allograft material is needed or a more suitable donor site should be chosen [9]. Additionally, alveolar cleft volume is also useful in predicting prognosis of ABG surgery [10, 11].

Three-dimensional imaging for individualized evaluation is currently recommended due to measurement inaccuracies of 2D imaging [12, 13]. Unlike most other pathologies, alveolar defects lack borders on certain sides, which complicates measurement. Therefore, the definition of boundary landmarks is especially critical to ensure consistent and reliable surgical practice and measurement. The authors believe that a clear definition of boundary landmarks is needed for true evidence-based surgery, and this review is presented as the first step to precisely define and achieve consensus on alveolar cleft boundaries.

Volumetric measurement of alveolar cleft requires particular software and specialised skills. Radiologists must have full information in order to properly decide on a suitable measurement method instead of being limited by the software they are familiar with. It is also anticipated that volumetric analysis and planning of ABG will be more commonplace in the future due to the ease provided by semi-automatic/automatic volumetric segmentation [14]. It is imperative that automated volumetric segmentation is created with evidence-based data and methodology, as proposed in this review.

Therefore, this review is intended to compile and evaluate information on different types of available workflows and landmarks for volumetric preoperative measurement of alveolar defects in cleft alveolus and palate, including innovations in AI. To our knowledge, this is the first review to evaluate them in detail to establish more standardized landmarks and protocols for future studies.

2. METHODS

The review was registered with the International Prospective Register of Systematic Reviews (PROSPERO ID: CRD42023479149) and conducted according to Preferred Reporting Items for Systematic Reviews and Meta-Analyses (PRISMA) [15]. The question posed in this review was: What expert-based and AI-based protocols are available for volumetric alveolar defect measurement in cleft alveolus and/or palate? The scope of the study was predetermined using the PICO framework. The population included patients with cleft alveolus and/or palate planned for alveolar bone graft. The intervention involved protocols utilising CT/CBCT images for measuring alveolar cleft defects by an expert or AI. For the comparison component, the scope encompassed no comparison, comparisons with other protocols (either by experts or AI), or comparisons with the actual graft volume. The outcome of the study focused on the preoperative three-dimensional measurement of alveolar defect that resulted in volumetric sizes, such as cm^3, mm^3, or ml. By incorporating studies that employed one or more measurement methods, this review provides a comprehensive overview of the available protocols. Further, discussions on the protocol in this review included workflow and landmarks associated with the measurement.

2.1. Eligibility Criteria

Inclusion criteria were cross-sectional research journal articles that reported defect volumetric size utilizing imaging data from CT or CBCT, focused on the protocols of preoperative volumetric measurements for alveolar bone graft in cleft cases, and were full text and written in English.

The exclusion criteria included studies involving syndromic cleft, gingiva- or periosteoplasty, and bone graft for purposes other than filling the alveolar defect in the cleft.

Studies were also excluded if they had no description of the workflow for volume measurement, involved simulated defect and animal models, and were published as review articles, case reports, case series, expert opinions, and conference poster abstracts. Additionally, protocols described in volumetric measurements to evaluate or compare clinical interventions and assessments of bone graft outcomes or post-operative assessments were considered a minor focus and, therefore, excluded.

2.2. Search Strategy

Searches were conducted on PubMed, Embase, and Scopus databases in November 2023, with access provided through the author's institution library access. Search strategies are listed in Table **1**, which were optimised based on the rules for the search engine of each database to obtain the most relevant articles and the least amount of non-relevant articles. MesH terms in PubMed and Emtree in Embase were included in the search strategy. Additional relevant articles were also hand-searched through Google Scholar and reference lists. Titles and abstracts were screened by two examiners following inclusion and exclusion criteria. Afterward, full-

text articles were retrieved and assessed for inclusion and exclusion by the same investigators. All reasons for exclusion were recorded. Consensus between the first, second, and third authors was sought if there was any ambiguity.

2.3. Data Extraction

The articles were noted for their inclusion and exclusion criteria, samples, patient characteristics, cleft type, study results, modality, workflow, anatomical landmarks of the defect borders, software and hardware, and reliability assessment by two investigators. The workflows were summarized by dividing them into several general types. They were all summarised, tabulated, noted if missing, presented, and discussed in the paper.

2.4. Study Quality Assessment

The quality appraisal tool, JBI Critical Appraisal Checklist for Analytical Cross-Sectional Studies [16], was used for quality assessment. Some of the parameters were modified for the study to clarify essential requirements for a robust and reproducible measurement protocol, specifically including assessments of the gold standard, reliability, and objective anatomical landmarks.

Q4 was considered positively assessed only if landmarks for the superior, inferior, and buccopalatal borders were clearly described. If either one or two sides of the borders were missing, they were considered unclear. Q7 received a positive assessment if all steps were specified with clarity that allowed for easy and unambiguous repetition. If there was no description of workflow, the study was excluded as part of the exclusion criteria. If multiple methods were addressed in the study, all methods were considered in unison for quality assessment.

3. RESULTS

3.1. Study Selection

A total of 1,594 titles and abstracts were imported into the Zotero reference manager (version 6.0.27) to be manually reviewed for duplicate removal. One study was flagged and retracted due to self-plagiarism, resulting in 233 articles. After reviewing titles and abstracts based on inclusion and exclusion criteria, 202 articles were removed. A total of 31 studies were read in full text, and 14 of them were excluded based on the same criteria. At the end of the study, 17 articles were included. The search process diagram is presented in Fig. (**1**).

3.2. Study Quality Assessment

The most common quality issues identified were a lack of comparison to the gold standard (only 24% of the studies were positively assessed in Q3a), lack of inter- and intra-observer reliability (29% in Q3b), and incomplete anatomical landmarks (24% in Q4) (Fig. **2**). It is worth noting that three studies failed to report reliable results despite having multiple observers/measurements, leading to questions about selective reporting [17-19].

3.3. Study Characteristics

A summary of the sampling methods, patient characteristics, cleft types, and main findings from all included studies is presented in Table **2**.

Table 1. Search strategy for each database.

-	PubMed	Embase	Scopus
#1	((cleft lip[MeSH Terms] OR "cleft palate"[MeSH Terms])) AND (("alveolar bone grafting"[MeSH Terms] OR "bone transplantation"[MeSH Terms]))	('cleft lip'/exp OR 'cleft palate'/exp) AND ('bone graft'/exp OR 'bone transplantation'/exp OR 'alveolar bone grafting'/exp OR 'alveolar bone'/exp OR 'alveolar bone defect'/exp)	(KEY(cleft AND lip) OR KEY(cleft AND palate) OR KEY (cleft AND lip AND palate)) AND (KEY(bone AND graft) OR KEY(alveolar AND bone AND graft*) OR KEY(bone AND transplant*))
#2	(Cleft lip* OR cleft palate*) AND (alveolar bone graft* OR bone transplant*)	(cleft* AND lip* OR (cleft* AND palate*)) AND (alveol* AND bone AND graft* OR (bone AND transplant*))	(TITLE-ABS-KEY(cleft* AND lip*) OR TITLE-ABS-KEY(cleft* AND palate*)) AND (TITLE-ABS-KEY(alveol* AND bone AND graft*) OR TITLE-ABS-KEY(bone AND transplant*))
#3	(3D OR 3-D OR three*dimension* OR cone*beam ct OR cone*beam computed tomography OR CBCT OR computed*tomography OR CT OR CT*scan)	(3D OR '3-D' OR three?dimension* OR (cone?beam AND ct) OR (cone?beam AND computed AND tomography) OR cbct OR computed?tomography OR ct OR ct?scan)	TITLE-ABS-KEY(3d) OR TITLE-ABS-KEY(3-d) OR TITLE-ABS-KEY(three dimension*) OR TITLE-ABS-KEY(cone beam ct) OR TITLE-ABS-KEY(cone beam computed tomography) OR TITLE-ABS-KEY(cbct) OR TITLE-ABS-KEY(computed tomography) OR TITLE-ABS-KEY(ct) OR TITLE-ABS-KEY(ct scan)
#4	(volume OR volumetric)	volum*	TITLE-ABS-KEY(volum*)
#5	(AI OR A.I OR artificial intelligence OR deep learning OR machine learning OR neural network OR CNN OR ANN OR support vector machine OR support vector network OR random forest OR decision tree)	(ai OR 'a.i' OR (artificial NEAR/2 intelligence) OR (deep NEAR/2 learning) OR (machine NEAR/2 learning) OR (neural NEAR/2 network) OR CNN OR ANN OR (support NEAR/2 vector NEAR/2 machine) OR (support NEAR/2 vector NEAR/2 network) OR (random NEAR/2 forest) OR (decision NEAR/2 forest))	(TITLE-ABS-KEY(AI) OR TITLE-ABS-KEY(A.I) OR TITLE-ABS-KEY(artificial AND intelligence) OR TITLE-ABS-KEY(deep AND learning) OR TITLE-ABS-KEY(machine AND learning) OR TITLE-ABS-KEY(neural AND network) OR TITLE-ABS-KEY(CNN) OR TITLE-ABS-KEY(ANN) OR TITLE-ABS-KEY(support AND vector AND machine) OR TITLE-ABS-KEY(support AND vector AND network) OR TITLE-ABS-KEY(random AND forest) OR TITLE-ABS-KEY(decision AND tree)
#6	#1 AND #3 AND #4	#1 AND #3 AND #4	#1 AND #3 AND #4
#7	#2 AND #3 AND #4	#2 AND #3 AND #4	#2 AND #3 AND #4
#8	#1 AND #3 AND #5	#1 AND #3 AND #5	#1 AND #3 AND #5
#9	#2 AND #3 AND #5	#2 AND #3 AND #5	#2 AND #3 AND #5

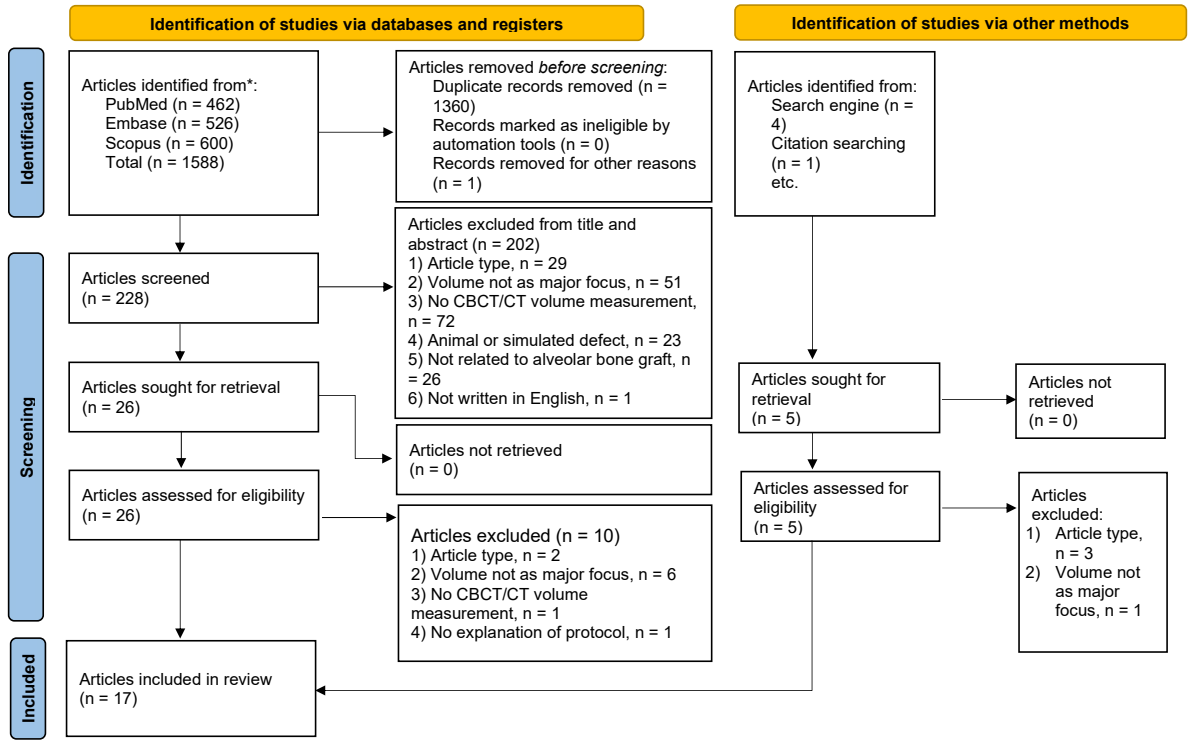

Fig. (1). Search process diagram.

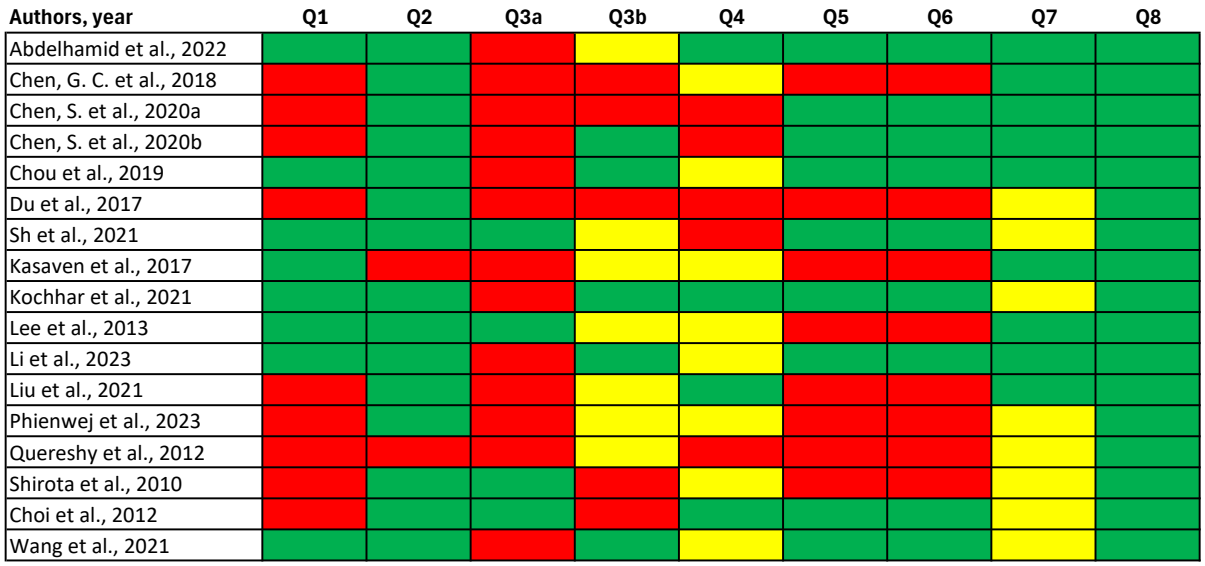

Q1: Were the criteria for inclusion in the sample clearly defined?; Q2: Were the study subjects and the setting described in detail?; Q3a: Was there an actual bone volume as gold standard to ensure measurement was done in a valid way?; Q3b: Was there intra- and interobserver reliability to ensure measurement was done in a reliable way?; Q4: Were objective, standard criteria (detailed anatomical landmarks) used for measurement of the condition?; Q5: Were confounding factors identified?; Q6: Were strategies to deal with confounding factors stated?; Q7: Was the workflow described in detail to establish how the outcome measurement was conducted?; Q8: Was appropriate statistical analysis used?; Green: Yes; Yellow: Unclear; Red: No.

Fig. (2). Quality assessment of included studies.

The average defect volume for unilateral cleft only, bilateral cleft only, and all types of clefts were 1.38 cm^3, 1.72 cm^3, and 1.61 cm^3, respectively. Most studies did not differentiate based on the involvement of the palate; therefore, the volumetric difference between CL and CLP could not be evaluated.

Table **3** summarises technical details, including modality, software and hardware, type of workflow, and anatomic landmarks. A total of 10 studies used CBCT [14, 19-27], and 7 studies used CT [5, 17, 18, 28-31]. Thirty workflows for alveolar defect volume measurement were found among 17 studies. Measurement by experts can be broadly divided into virtual and 3D printing methods. The most often used workflow for virtual measurement was manual segmentation in each axial slice [5, 17, 19, 20, 22, 24, 25, 27-31], followed by orthogonal tracing or editing [19, 21], mirrored template using automatic superimposition [18, 31], geometric estimation [26], region growing [23], and custom algorithms [23]. Most of the studies used commercial medical image segmentation, analysis, and design software (Mimics, Materialise, Leuven, Belgium) for virtual measurements. With 3D printing, 6 studies printed the patient's maxilla [17, 18, 21, 25, 28, 30], while one study made a physical model of the defect itself [23]. One additional study investigated the use of artificial intelligence through a 3D U-Net architecture for segmentation and measurement [14].

Table 2. Summary of included studies.

Author, Year	Sample Size (Sampling Technique)	Cleft Type	Patient Characteristics	Main Findings
Shirota *et al.*, 2010 [19]	13	UCL UCLP BCL BCLP	- 61.5% males, 38.5% females - Mean age 22.10 years - 76.9% unilateral cleft lip and palate, 15.4% bilateral cleft lip and palate, 7.7% unilateral cleft lip and alveolus	Average volume (3.8 ± 0.8 cm^3), average volume of gold standard (3.5 ± 0.8 cm^3), comparison with gold standard not statistitically significant and closely correlated
Choi *et al.*, 2012 [5]	47	UCL UCLP BCL BCLP	- 61.7% males, 38.3% females - Mean age 9.8, ranged 8 - 11 years - Unilateral cleft lip and alveolus 27.6% - Unilateral cleft lip and palate 38.3% - Bilateral cleft lip and alveolus 4.3% - Bilateral cleft lip and palate 29.8%	Average volume (1.2 ± 0.4 cm^3), average volume of gold standard (1.3 ± 0.5 cm^3), unilateral *vs* bilateral cleft, comparison with gold standard. (Intraobserver reliability result were not reported despite having multiple measurements)
Quereshy *et al.*, 2012 [26]	14 (randomised)	UCL UCLP	not specified (all demographic data were anonymized for the investigators)	Average volume (0.4890 ± 0.1516 cm^3); intraobserver ICC for cleft width: 0.879, cleft height: 0.827, cleft length: 0.305
Lee *et al.*, 2013 [24]	7	Complete UCLP	- 42.86% males, 57.14% females - Mean age 11.4 ± 2.0 years, ranged 8.8 - 14.8 years	Average volume (2.4 ± 1.2 cm^3), interobserver ICC > 0.90, average volume of gold standard (2.5 ± 1.3 cm^3), difference with gold standard
Du *et al.*, 2017 [18]	10	UCL UCLP	- 70% males, 30% females - age ranges 8-12 years - 60% cleft lip and palate, 40% cleft lip only	Average volume and difference (A: 1.47 cm^3; B: 1.52 cm^3). (Interobserver and intraobserver reliability result were not reported despite having multiple observers and measurements)
Kasaven *et al.*, 2017 [23]	15 (consecutive)	UCLP	not specified	Average volume and difference (A: 0.57556 cm^3; B: 0.54043 cm^3; C: 0.66262 cm^3)
Chen, G. C. *et al.*, 2018 [29]	10	UCLP	- 70% males, 30% females - age ranges 8-12 years	Average volume (1.81197 ± 0.81790 cm^3), time, correlation between volume and time
Chou *et al.*, 2019 [21]	32 (consecutive, determined by sample size calculation)	UCL BCL	68.75% unilateral cleft, of which 59.1% is male and 40.9% is female. Mean age is 9.1 ± 0.2 years 31.25% bilateral cleft, of which 60% is male and 40% is female. Mean age is 9.6 ± 0.7 years	Average volume unilateral (A: 1.09 ± 0.25 cm^3; B: 1.09 ± 0.24 cm^3) *vs* bilateral cleft (A: 2.02 ± 0.27 cm^3; B: 2.05 ± 0.22 cm^3), volume difference, Intraobserver ICC method A (0.824-0.838) and method B (0.765-0.896), interobserver ICC method A (0.650- 0.769) and method B (0.7699-0.873)

(Table 2) contd.....

Author, Year	Sample Size (Sampling Technique)	Cleft Type	Patient Characteristics	Main Findings
Chen, S. *et al.*, 2020a [17]	12	BCL BCLP	- 66.6% males, 33.3% females - age ranges 8-11 years - 75% cleft lip and palate, 25% cleft lip only	Average volume (A: 1.52 cm^3; B: 1.45 cm^3), volume left *vs* right, time. (Interobserver and intraobserver reliability result were not reported despite having multiple observers and measurements)
Chen, S. *et al.*, 2020b [28]	10	UCL UCLP	- 70% males, 30% females - age ranges 8-13 years - 80% cleft lip and palate, 20% cleft lip only	Average volume and difference (A: 1.42 cm^3; B: 1.39 cm^3), intraobserver ICC: 0.95 - 0.97, Interobserver ICC: 0.94 - 0.98, time
Kochhar *et al.*, 2021 [27]	31 (determined by sample size calculation)	UCL UCLP	- 54.8% males, 45.2% females - Mean age 11 ± 0.98 years, ranged 8-12 years - 58% unilateral cleft on right side, 42% unilateral cleft on left side	Average volume between non-oriented (Left: 2.26 ± 1.16 cm^3; Right: 1.75 ± 0.69 cm^3) and oriented (Left: 2.73 ± 1.27 cm^3; Right: 2.25 ± 0.72 cm^3), left *vs* right, difference, intraobserver ICC ≥ 0.90, interobserver ICC ≥ 0.80
Liu *et al.*, 2021 [31]	20	UCL UCLP	- 65% males, 35% females - Age ranged 8-12 years - 70% cleft lip and palate, 30% cleft lip	Average volume (A: 1.27 ± 0.35 cm^3; B: 1.23 ± 0.32 cm^3), interobserver ICC method A: 0.966 and method B: 0.980
Sh *et al.*, 2021 [22]	20 (convenience sampling, determined by sample size calculation)	UCL UCLP	- 40% males, 60% females - Mean age 10 ± 1.02 years	Average volume by expertise and slice thickness (radiologist: 1.15; 1.14; 1.14 cm^3, surgeon: 1.17 cm^3), volume by gold standard (1.08 ± 0.60 cm^3), difference to gold standard statistically significant
Wang *et al.*, 2021 [14]	60 Group 1: 30 samples for expert measurement and development of AI (training: 24; validation: 3; testing: 3) Group 2: 30 samples for evaluation by AI	UCLP	- 65% males, 35% females - Mean age 11.52 ± 3.27 years, ranged 8 - 18 years) - 68.3% unilateral left defect, 31.5% unilateral right defect	Average volume (1.24 ± 0.29 cm^3), height *vs* width *vs* length, intraobserver ICC method A: > 0.90, interobserver measurements were not statistically different (p = 0.39), similarity (Dice coefficient)
Abdelhamid *et al.*, 2022 [20]	12	UCL UCLP	- 58% males, 42% females - 50% unilateral left alveolar cleft, 50% unilateral right alveolar cleft - Mean age 10.6 +/- 2.1	Average volume (A: 1.19 ± 0.04 cm^3; B: 1.17 ± 0.04 cm^3) and difference, interobserver ICC method A: 0.998 and method B: 0.626, time
Li *et al.*, 2023 [30]	100 (randomised)	UCL UCLP	- 61% males, 39% females - Mean age 19.32 years, ranged 13-42 years	Average volume (A: 1.55 ± 0.42 cm^3; B: 1.58 ± 0.41 cm^3), intraobserver ICC (both methods): 0.98 - 0.99, interobserver ICC (both methods): 0.95 - 0.99, time
Phienwej *et al.*, 2023 [25]	20	UCLP	- 65% males, 35% females - Mean age 12.10 ± 3.92 years, ranged 8-20 years	Average volume (A: 1.00 ± 0.31 cm^3; B: 1.03 ± 0.31 cm3), mean difference, Intraobserver ICC method A: 0.996 and method B: 0.949

Abbreviations: UCL: Unilateral cleft lip and alveolar, UCLP: Unilateral cleft lip and palate, BCL: Bilateral cleft lip and alveolar, BCLP: Bilateral cleft lip and palate.

Various anatomical landmarks were described in the literature (Table **3**). Six studies provided a complete description of virtual landmarks for superior, inferior, and buccopalatal boundaries of the alveolar cleft [5, 20, 21, 25, 27, 31]. Six studies only included partial virtual landmarks [17, 18, 22, 26, 28], whereas 5 others offered none [13, 14, 18, 22, 24]. Only one landmark description was described for 3D printing [25]. None were needed for AI.

Additionally, 4 studies showed comparisons to actual graft volume, which varied from measuring the actual graft intra-operatively [5, 19] to making impressions during surgery [22] or imaging 1 month after surgery [14]. Intra-class correlation coefficient (ICC) measurements for reliability ranged from 0.305 – 0.80.

4. DISCUSSION

This systematic review aimed to investigate existing protocols for the three-dimensional measurement of alveolar defects in individuals with cleft alveolus and palate. Most ABG surgeries are conducted with autologous bone material. Therefore, accurate determination of the defect volume

before bone harvesting is important to achieve optimal outcomes with minimal morbidity [4, 5]. Overharvesting leads to an increased risk of morbidity, such as infection, hematoma, bleeding, nerve injury, fracture, and extended hospitalization [21, 32]. Conversely, underfilling of the defect could lead to the failure of canine eruption, failed orthodontic movement or implant placement, and compromised facial aesthetics due to reduced bony support [1, 33]. The amount of bone graft used is directly proportional to the alveolar bone graft success [11]. Some studies have reported success with synthetic or allograft materials, where preoperative volume determination also aids in thorough planning, ensuring cost-effectiveness, and reducing operator dependency [34, 35].

Detailed discussions on the protocol in this review include workflow and landmarks. These workflows can be generally divided into virtual and 3D-printing workflows, which are described below. Only one study that explored AI was found in this review, which was published in 2021. This is consistent with the rising development of AI in general [36]. Recent developments in deep learning have enabled complex imaging tasks that were previously impossible with conventional or older AI technologies [36]; hence, more studies involving AI are expected to emerge in the future.

More than half of the studies were published within 3 years of the article search, indicating an increased desire to optimise the utilisation of 3D imaging beyond simple visual assessment or linear measurements. While the majority of the studies used CBCT, about 41% used CT. Additionally, discussions on the measurement accuracy associated with modality, X-ray parameters, voxel size, and slice thickness are outside the scope of the review. However, studies have shown that larger bony anatomical structures, such as cleft, are equally visible and dimensionally accurate in both modalities [37-39]. For these reasons, we consider the protocols described in this review to be viable for both modalities with various parameters.

Table 3. Technical details of the studies.

Author, Year	Modality	Software and Hardware	Summary of Workflow	Anatomical Landmarks
Abdelhamid *et al.*, 2022 [20]	CBCT	A: OnDemand3D (Cybermed Inc., Seoul, South Korea)	A: traced axially slice by slice	S: ANS level I: CEJ of tooth mesial to the cleft M/D: cleft borders L: continuity of mesiolabial and distolabial dentoalveolar margins P: continuity of mesiopalatal and distopalatal bony margins
		B: InVesalius 3 (CTI, Campinas, Brazil)	B: traced axially slice by slice	
Chen, G. C. *et al.*, 2018 [29]	CT	Mimics (Materialise, Leuven, Belgium)	Traced axially slice by slice, subtracting maxilla	L: a line connecting mesial and distal alveolar segments P: a line connecting mesial and distal alveolar segments
Chen, S. *et al.*, 2020a [17]	CT	A: Mimics	A: traced axially slice by slice, subtracting maxilla	-
		B: Mimics + Mass Portal XD30 (Mass Portal SIA, Riga, Latvia)	B: 3D-printing of maxilla, water displacement technique	-
Chen, S. *et al.*, 2020b [28]	CT	A: Mimics	A: traced axially slice by slice, subtracting maxilla	-
		B: Mimics + Mass Portal XD30	B: 3D-printing of maxilla, water displacement technique	-
Chou *et al.*, 2019 [21]	CBCT	A: SimPlant Pro (Materialise Dental, Leuven, Belgium)	A: traced orthogonally	S: plane between ANS up-tilted to the lateral segments I: plane between CEJs L/P: continuity to the maxillary arch
		B: Objet30 OrthoDesk 3D Printer, (Stratasys, Rehovot, Israel)	B: 3D-printing of maxilla, water displacement technique	-
Du *et al.*, 2017 [18]	CT	A: Mimics for STL conversion; Geomagic Studio 2013 (Geomagic, Morrisville, USA)	A: Mirrored template	-
		B: Mimics + Zprinter 350 (Z Corporation, Burlington, USA)	B: 3D-printing of maxilla, water displacement technique	-
Sh *et al.*, 2021 [22]	CBCT	A: OnDemand 3D	A: traced axially slice by slice	-
		B: -	B: Intra-operative gold standard, using silicone impression material	-
Kasaven *et al.*, 2017 [23]	CBCT	A: MATLAB (The Mathworks Inc, Natik, USA)	A: semiautomatic algorithm, axial slice by slice	S: slice in which the alveolar defect was first seen I: slice in which bifurcation of first molar was seen in cleft side
		B: Volume Graphics Studio Max 2.2 (Volume Graphics, Heidelberg, Germany)	B: region growing, axial slice by slice	
		C: Mimics; CatalystEx 4.2 (Stratasys, Eden Prairie, USA); Dimension Printing (Stratasysinc, Eden Prairies, Minnesota, USA); microCT X-Tek BT 160 UF (Nikon Metrology X-Tek Systems Ltd, Tring, UK)	C: 3D-printing of defect, volume measured with microCT	-

(Table 3) contd.....

Author, Year	Modality	Software and Hardware	Summary of Workflow	Anatomical Landmarks
Kochhar *et al.*, 2021 [27]	CBCT	Osirix (Pixmeo Inc., Genève, Switzerland)	A: traced axially slice by slice, non-oriented	S: at sight of bone defect I: CEJ of teeth adjacent to the defect M/D: margin of the cleft L: following the contour of the contralateral side P: following the contour of the contralateral side
			B: traced axially slice by slice, oriented	
Lee *et al.*, 2013 [24]	CBCT	Dolphin Imaging Version 11.0.3.9 (Dolphin Imaging, Chatsworth, USA); XnView (XnSoft, Reims, France); SkyScan Dataviewer (Bruker-microCT, Kontich, Belgium)	A: traced axially slice by slice	S: ANS I: inferior border of alveolar crest
			B: Post-operative gold standard from CBCT imaging (steps not specified)	-
Li *et al.*, 2023 [30]	CT	A: Mimics	A: multiple slice edit, subtracting maxilla	S: most inferior part of piriform aperture at non-cleft side I: CEJ of central incisor
		B: Mimics; Mass Portal XD30	B: 3D-printing of maxilla, water displacement technique	-
Liu *et al.*, 2021 [31]	CT	A: Mimics; Geomagic Wrap 2017	A: mirrored template, subtracting maxilla	Not needed (automatic superimposition)
		B: Mimics	B: traced axially slice by slice, subtracting maxilla	S: 6 slices (3 mm) inferior to ANS, parallel to reference plane I: A plane parallel to greater palatine foramens and CEJ of buccal surface central incisor on the cleft side. Also serves as reference plane. L/P: following outlines of contralateral side
Phienwej *et al.*, 2023 [25]	CBCT	A: Mimics v.17	A: traced multiple slices axially	S: plane from ANS, most lateral and inferior point of pyriform aperture in cleft side, and the most superior point of mesiopalatal margin of the lateral alveolar segment I: plane from inferior of mesiolabial margin of the medial alveolar segment, inferior of mesiolabial margin of the lateral alveolar segment, inferior of mesiopalatal margin of the medial alveolar segment M/D: margins of the cleft L: linear line connecting the labial edges of the alveolar segments P: linear line connecting the palatal edges of the alveolar segments
		B: Mimics v.17); Form 2 3D printer (Formlabs Inc., Massachusetts, USA)	B: 3D-printing of maxilla, water displacement technique	S: same as method A I: same as method A
Quereshy *et al.*, 2012 [26]	CBCT	InVivo (Anatomage Inc, San Jose, USA)	Geometric estimation	-
Shirota *et al.*, 2010 [19]	CBCT	A: SimPlant Pro ver. 8.1	A: traced axially, edited orthogonally	S: inferior margin of anterior nasal aperture I: inferior margin of alveolar bone adjacent to the defect
		B: -	B: Intraoperative actual bone volume using syringe method	-
Choi *et al.*, 2012 [5]	CT	A: Radipia 3D 2.8 (Infinitt Healthcare, Seoul, South Korea)	A: traced axially slice by slice	S: floor of pyriform aperture I: alveolar crest of adjacent alveolar segments L/P: the labiopalatal dimension was made as thick as the adjacent normal alveolar bone
		B: Ondemand 3D 1.0	B: traced axially slice by slice	
		C: -	C: Intraoperative actual bone volume using syringe method	-
Wang *et al.*, 2021 [14]	CBCT	A: ITK-Snap (Penn Image Computing and Science Laboratory, Philadelphia, USA))	A: manual and semi-automatic segmentation	L/P: following the contour of contralateral maxillary arch
		B: PyTorch, 3D U-Net	B: AI Deep learning	Not needed

Abbreviations: S: superior, I: inferior, L/P: labiopalatal, M/D: mesiodistal.

Current studies revealed that the determination of landmark of cleft boundaries was seen as a low priority and was rarely reported. Precise operational definition of each landmark is crucial to reduce errors [40]. Therefore, this article is intended to help future researchers formulate precise and appropriate landmarks for alveolar cleft defect measurement.

4.1. Evaluation of Workflow for Virtual Measurements

The most commonly used workflow involved manually tracing the defect boundaries slice by slice in the axial view [5, 17, 20, 22, 24, 27-29, 31]. This technique is simple although possibly tedious, but can be achieved by a lot of software programs. Manual tracing has been tested against actual bone volume with clinically acceptable accuracy. Due to the manual nature of this technique, reproducibility is of particular concern. The studies utilising various software reported reliability ICC values ranging from 0.626-0.980 [5, 20, 24, 25, 27, 28, 30, 31].

An open-sourced software (Invesalius, CTI, Campinas, Brazil), which tends to be harder to use, was an outlier [20], presenting significantly worse reliability. Excluding this software, the reliability for axial tracing was at least 0.80. This indicates that the choice of software must also be considered, and it is best to use software programs that have been validated for clinical use.

Based on the findings in this review, commercial medical image processing software (Mimics, Materialise, Leuven, Belgium) offers multiple methods and has a reasonable amount of supporting evidence. Multiple-slice tracing was also used to accelerate the measurement process. However, both studies that used multiple-slice tracing did not mention the spacing distance between traced slices. Nevertheless, tracing in the axial slice seemed to be an adequately reliable method based on available evidence, although more studies are needed to confirm its accuracy.

Two studies evaluated a dental implant planning software (SimPlant Pro, Dentsply Sirona, Charlotte, USA) using manual orthogonal tracing or editing [19, 21]. Reported reliability was suboptimal, with intraclass correlation coefficients ranging from 0.650 to 0.838. However, the workflow and anatomical landmarks in the virtual method were described with good clarity. Based on these results and missing reliability data, orthogonal tracing or editing with this implant planning software could not be advocated at present due to the lack of evidence.

Mirroring the maxilla to use as a template in unilateral cases was explored in two studies, and both used automated superimposition [18, 31]. A personalised template made from the patient's anatomy has the potential to reduce operator variability in shaping optimal alveolar shape in filling the defect, especially using automated superimposition. However, asymmetry of the nasal pyriform associated with unilateral clefts potentially complicates superimposition. Although there is no comparison to actual graft volume, this review found comparable accuracy to tracing slice-by-slice and 3D printing [18, 31]. However, reporting must be improved, especially in terms of reliability and comparison to actual graft volume.

Quereshy *et al*. measured defect width, height, and thickness to estimate volume using a geometric formula [26]. Intraobserver ICC was poor for defect thickness (0.305). Workflow and landmark anatomy were both unclear, which may have contributed to decreased reliability. Additionally, the measurements seemed to have been identified from a 3D-rendered virtual model rather than from sliced images, which decreases accuracy.

Barbosa *et al*. also found that simple geometric estimation is significantly inaccurate compared to true volumetric measurements [32]. Consequently, this technique should be avoided.

Semi-automatic techniques were used in two studies [14, 23]. Kasaven *et al*. explored a region-growing tool and a custom algorithm with industrial and materials science image analysis software (Volume Graphics Studio Max, Hexagon, Stockholm, Sweden) and a programmable image processing and analysis software (MATLAB, The MathWorks, Inc., Natick, USA), respectively [23]. These two techniques are highly dependent on density boundaries; thus, they have limited suitability to cleft images and require significant manual refinement. Wang *et al*. used a combination of manual and semi-automatic processes in an open-source medical image segmentation software (ITK-Snap, Penn Image Computing and Science Laboratory, Philadelphia, USA) [14]. However, the lack of clarity in the workflow described by Wang *et al*. left some uncertainty in the exact tools used. The study reported 10 hours of work per CBCT, which is a considerable difference from the minutes of work reported with other software (Mimics, Materialise, Leuven, Belgium) [20]. Therefore, time *versus* cost might be an important consideration in deciding which software to use. Currently, there is not enough evidence to promote these semi-automatic techniques for clinical purposes.

Wang *et al*. also investigated AI technology by using 3D U-Net, an AI architecture based on convolutional neural network [14]. The architecture was designed to work with small training datasets and large images, specifically to segment medical images [41]. During the training of the AI system, Wang *et al*. split each CBCT image into patches in the sliding window technique to be trained and create an output of labels for the segmentation. Optimization was done *via* generalised dice loss [14]. The similarity of AI segmentation compared to manual segmentation was 0.77 +/- 0.06, which was considered moderate to high [42]. Several other studies have also recently used AI for cleft [43, 44]. The use of AI for identifying and measuring the volume of alveolar cleft is promising, and further development is needed. It should be noted that to have any clinical value. AI systems must be developed using evidence-based data and applied under the supervision and approval of clinicians.

4.2. Evaluation of Workflow for 3D Printing

3D printing itself has been established to have adequate accuracy for medical and dental use [45, 46]. For alveolar cleft measurement, typically, plasticine was filled by observers into a 3D-printed skull. Thus, measurement was based on the plasticine filling rather than any 3D-printed object. The printed skull itself may be useful for education or precise, personalised planning [47, 48]. An exception to this was the research by Kasaven *et al*., in which a defect-shaped

object was printed. This protocol could create 3D-printed biomaterial or scaffold [49] to aid alveolar bone graft surgery in addition to mere measurement. The time required for the 3D printing method was consistently longer than virtual measurements [17, 28, 30], which could be a significant drawback. Although cost was not part of the research from any of the included studies, it should also be part of consideration when choosing the technique.

In terms of cleft volume measurement by 3D-printed methods, this review found comparable accuracy to many types of virtual workflow, such as axial tracing [17, 25, 28, 30], orthogonal tracing [21], mirrored template [18], and region-growing techniques [19]. Yet, no studies were found that compared 3D printing-based cleft measurement to actual bone graft volume. Reported reliability ranged from 0.765 to 0.949 [23, 25, 28], although two studies did not provide reliable data [17, 18]. One study found moderate interobserver reliability between 2 cleft surgeons [21]. This was possibly due to the absence of defined landmarks for cleft filling in all 3D-printed protocols, except for the one proposed by Phienwej *et al*., who created superior and inferior boundaries for the defect, printed as part of the skull model [25]. While this attempt was appreciated, such physical boundaries would not be useful if the maxilla model is to be used as a simulation for surgery due to altered anatomy. Even though the research was done on 3D-printed objects, the fact that suboptimal reliability was found between cleft surgeons using physical models [21] could be significant. An argument could be made that this unreliability could extend to the surgery itself, supported by studies that found operator dependency of alveolar bone graft surgery [50, 51] and evidence of under- or overfilling [4, 5].

Additionally, literature on alveolar bone graft surgery frequently gives little description of landmarks or guidance for adequate defect filling. This highlights the importance of preoperative cleft volume measurements to guide surgeons and reduce operator dependency. Nonetheless, 3D printing for cleft care is promising and warrants future exploration with particular regard to landmark description and reliability.

4.3. Landmarks

Landmarks to determine borders of the alveolar defect should preferably be reliable, fast, and easy to determine. More importantly, they should have clinical significance and be compatible with good functional and aesthetic outcomes. Landmarks chosen for pre-operative determination of defect borders should reflect landmarks seen during surgery. However, none of the studies that provided a complete protocol for anatomical landmarks in this review had a comparison to actual bone volume.

In the current review, five studies used Cemento-enamel Junction (CEJ) [20, 21, 27, 30, 31], and another four used alveolar ridge [5, 19, 24, 25] as landmarks for the inferior margin. The normal alveolar ridge is 1-2 mm below CEJ and even farther in periodontitis or in cases of the alveolar cleft with bone dehiscence. CEJ has the advantage of being relatively constant and easily recognizable in imaging. Normal bone height and CEJ are both used as benchmarks for success evaluation [6, 52-55] and are agreeable with one another [56]. Therefore, CEJ may be preferable as a landmark for the inferior margin of alveolar defect.

For the superior margin, four studies used landmarks associated with the Anterior Nasal Spine (ANS) [19-21, 24], and two studies used a base of pyriform aperture [5, 30]. Phienwej *et al*. used both landmarks, describing the superior limit as a plane defined by ANS, the most lateral and inferior point of the pyriform aperture on the cleft side, and the most superior point of the mesiopalatal margin of the lateral alveolar segment [25]. Liu *et al*. set the superior limit at 3 mm below ANS [31]. Both ANS and pyriform aperture have been reported in the literature to be used as surgical landmarks and success measures [6, 57-61]. In cleft cases, the base of the pyriform aperture is harder to identify because it is absent in a complete alveolar defect and often asymmetrical compared to the normal side in unilateral clefts. ANS, as the superior limit, has the most supporting evidence and may be more desirable.

Alveolar thickness and shape may be of concern in the labio-palatal dimension. Three studies followed the contour of the contralateral side [14, 27, 31], two studies followed the continuity of the maxillary arch [20, 21], and another two studies used straight lines connecting the alveolar segments [25, 29]. One study prioritised thickness by dictating the defect filling to have equal thickness with adjacent alveolar segments [5]. However, not many studies evaluating volumetric ABG outcomes have described labio-palatal margins. Nagashima *et al*. [62] used a mirror image of the contralateral side as a benchmark for the outcome, while Kibe *et al*. [34] used a tangent line connecting the labial and palatal edges of the defect [34, 62]. As long as good continuity of the arch is achieved, literature is sparse to determine if graft shape (contoured *versus* straight line) affects functional or facial aesthetic outcomes. Additionally, the choice between ideal contour and straight lines might also be practical as some software may not be able to create contoured lines.

Furthermore, the majority of the studies have used graft thickness as a success measure. Padwa *et al*. determined graft success if the labio-palatal thickness of the graft is ≥75% of adjacent tooth root width [6]. Stasiak *et al*. determined a moderate outcome if the thickness is ≥50% - ≤100% of central incisor root width and a good outcome if the thickness is ≥100% [11]. Ideally, it should be at least 8 mm thick to accommodate the size of canines [33]. To comply with the outcome assessment, we recommend prioritizing good continuity with the arch and appropriate thickness as labiopalatal guidance.

Creating planes for defect limit would be more time-consuming than point landmarks, and current evidence does not clearly indicate whether it improves reliability. Point landmarks would be faster and easier to create but are more prone to patient positioning errors. One study reported that non-oriented and oriented data had equal performance [27]. With current studies, there is no evidence to discourage the use of point landmarks.

Among articles that used 3D printing, only one study attempted to provide some guidance for identifying the borders of the filling [25]. Planning the operational definition of ana-

tomical landmarks for the defect borders is important to obtain the most reliable measurements. Although most of the reported reliability was good to excellent, a lot of the inter- and/or intraobserver reliability data in these studies were incomplete. In this regard, standardisation of border landmarks would create comparability between studies. Therefore, future studies with more thorough reporting of the landmarks and reliability are needed.

4.4. Limitations

Several studies were identified that included indirect comparisons to actual bone volume, but the validity of these appointed gold standard measurements was out of the scope of this study. Factors such as modality, X-ray parameters, voxel size, and slice thickness were also not evaluated in detail. However, evidence has shown that the choice of modality (CT and CBCT) and parameters do not significantly affect measurements of large structures, such as cleft [37, 63]. While some aspects of treatment flow (such as time and cost) were briefly discussed in the review, this aspect is rarely discussed in the studies, especially in regard to the surgery itself. Moreover, further research is needed to address important deficiencies in the current literature, such as investigating the validity and accuracy of each measurement method, reliability, and standardising landmarks to ensure volume comparability between studies.

Furthermore, the influence of preoperative volume determination on treatment flow and surgical consistency must be covered in areas of investigation. Recommendations in this review are based on available literature and professional judgement from experts with decades of experience; however, some aspects still require further evidence. Other factors that may impact surgical success and consistency are beyond the scope of this review. Nevertheless, the findings of this review would be important to pinpoint gaps in current knowledge and establish more standardized landmarks and protocols for future studies.

CONCLUSION

Diverse protocols for measuring the volume of alveolar defects in cleft alveolus and/or palate are available in the literature, employing various workflow and anatomical landmarks. The workflow with the most supporting evidence is manual tracing in the axial slice. Landmarks advocated by this review are CEJ, ANS, and continuity with the alveolar segments exhibiting adequate labio-palatal thickness as superior, inferior, and labio-palatal borders, respectively. Additionally, studies using AI to help measure alveolar defect volume are emerging and need to be explored.

The absence of a widely accepted consensus for the preoperative volumetric measurements of alveolar defect in cleft alveolus and/or palate has been observed in this review. Thus, the creation of valid, reliable, and standardized guidelines is needed for clinical and research applications of alveolar cleft volume. To help create a technical guideline, future studies must consider methodological and reporting quality as a priority, especially regarding the presence of gold standard, inter- and intraobserver reliability, and complete description of anatomical landmarks.

AUTHORS' CONTRIBUTIONS

The authors confirm their contribution to the paper as follows: I.S., M.P., N.N., and H.S.: Study conception and design; I.S., M.P., and B.K.: Data collection; I.S., M.P., N.N., D.A., and B.K.: Analysis and interpretation of results; and I.S., M.P., N.N., and H.S.: Draft manuscript. All authors reviewed the results and approved the final version of the manuscript.

LIST OF ABBREVIATIONS

AI	=	Artificial Intel
ABG	=	Alveolar Bone Graft
ANS	=	Anterior Nasal Spine
CEJ	=	Cemento-enamel Junction
CL	=	Cleft Lip
CPL	=	Cleft Lip and Palate
CT	=	Computed Tomography
CBCT	=	Cone-beam Computed Tomography
	=	

CONSENT FOR PUBLICATION

Not applicable.

STANDARDS OF REPORTING

PRISMA guidelines and methodology were followed.

AVAILABILITY OF DATA AND MATERIALS

The data supporting the findings of the article will be available from the corresponding author [I.S] upon reasonable request.

FUNDING

This study was financially supported by the University of Indonesia, Indonesia (NKB-663/UN2.RST/HKP.05.00/2024).

CONFLICT OF INTEREST

The authors declare no conflict of interest, financial or otherwise.

ACKNOWLEDGEMENTS

The authors would like to acknowledge Universitas Indonesia, Indonesia (NKB-663/UN2.RST/HKP.05.00/2024) for supporting the publication fees of this article.

SUPPLEMENTARY MATERIAL

PRISMA checklist is available on the publisher's website as supplementary material.

REFERENCES

[1] Berkowitz S. Cleft Lip and Palate. Berlin, Heidelberg: Springer 2013. http://dx.doi.org/10.1007/978-3-642-30770-6

[2] Salari N, Darvishi N, Heydari M, Bokaee S, Darvishi F, Mohammadi M. Global prevalence of cleft palate, cleft lip and cleft palate and lip: A comprehensive systematic review and meta-

analysis. J Stomatol Oral Maxillofac Surg 2022; 123(2): 110-20. http://dx.doi.org/10.1016/j.jormas.2021.05.008 PMID: 34033944
[3] Mahardawi B, Boonsiriseth K, Pairuchvej V, Wongsirichat N. Alveolar cleft bone grafting: Factors affecting case prognosis. J Korean Assoc Oral Maxillofac Surg 2020; 46(6): 409-16. http://dx.doi.org/10.5125/jkaoms.2020.46.6.409 PMID: 33377466
[4] Suomalainen A, Åberg T, Rautio J, Hurmerinta K. Cone beam computed tomography in the assessment of alveolar bone grafting in children with unilateral cleft lip and palate. Eur J Orthod 2014; 36(5): 603-11. http://dx.doi.org/10.1093/ejo/cjt105 PMID: 24509615
[5] Choi HS, Choi HG, Kim SH, *et al*. Influence of the alveolar cleft type on preoperative estimation using 3d ct assessment for alveolar cleft. Arch Plast Surg 2012; 39(5): 477-82. http://dx.doi.org/10.5999/aps.2012.39.5.477 PMID: 23094242
[6] Padwa BL, Tio P, Garkhail P, Nuzzi LC. Cone beam computed tomographic analysis demonstrates a 94% radiographic success rate in 783 alveolar bone grafts. J Oral Maxillofac Surg 2022; 80(4): 633-40. http://dx.doi.org/10.1016/j.joms.2021.12.004 PMID: 34990600
[7] Jahanbin A, Kamyabnezhad E, Raisolsadat MA, Farzanegan F, Bardideh E. Long-term stability of alveolar bone graft in cleft lip and palate patients: Systematic review and meta-analysis. J Craniofac Surg 2022; 33(2): e194-200. http://dx.doi.org/10.1097/SCS.0000000000008254 PMID: 35385241
[8] Virani FR, Chua EC, Timbang MR, Hsieh T, Senders CW. Three-dimensional printing in cleft care: A systematic review. Cleft Palate Craniofac J 2022; 59(4): 484-96. http://dx.doi.org/10.1177/10556656211013175 PMID: 33960208
[9] Shirzadeh A, Rahpeyma A, Khajehahmadi S. A prospective study of chin bone graft harvesting for unilateral maxillary alveolar cleft during mixed dentition. J Oral Maxillofac Surg 2018; 76(1): 180-8. http://dx.doi.org/10.1016/j.joms.2017.07.143 PMID: 28774851
[10] Roohani I, Youn S, Alfeerawi S. Failure rates based on alveolar cleft volume: An analysis of the critical-sized defect for alveolar bone grafting. Plast Reconstr Surg 2024; 155(2): 377e-86e. http://dx.doi.org/10.1097/PRS.0000000000011503 PMID: 38684030
[11] Stasiak M, Wojtaszek-Słomińska A, Racka-Pilszak B. A novel method for alveolar bone grafting assessment in cleft lip and palate patients: Cone-beam computed tomography evaluation. Clin Oral Investig 2021; 25(4): 1967-75. http://dx.doi.org/10.1007/s00784-020-03505-z PMID: 32803441
[12] De Mulder D, Cadenas de Llano-Pérula M, Willems G, Jacobs R, Dormaar JT, Verdonck A. An optimized imaging protocol for orofacial cleft patients. Clin Exp Dent Res 2018; 4(5): 152-7. http://dx.doi.org/10.1002/cre2.123 PMID: 30386636
[13] Barbosa GL, Emodi O, Pretti H, van Aalst JA. GAND classification and volumetric assessment of unilateral cleft lip and palate malformations using cone beam computed tomography. Int J Oral Maxillofac Surg 2016; 45(11): 1333-40. http://dx.doi.org/10.1016/j.ijom.2016.05.008 PMID: 27288267
[14] Wang X, Pastewait M, Wu TH, *et al*. 3D morphometric quantification of maxillae and defects for patients with unilateral cleft palate *via* deep learning-based CBCT image auto-segmentation. Orthod Craniofac Res 2021; 24 Suppl 2(Suppl 2): 108-16. http://dx.doi.org/10.1111/ocr.12482 PMID: 33711187
[15] Page MJ, McKenzie JE, Bossuyt PM, *et al*. The PRISMA 2020 statement: An updated guideline for reporting systematic reviews. BMJ 2021; 372(71): n71. http://dx.doi.org/10.1136/bmj.n71 PMID: 33782057
[16] Moola S, Munn Z, Tufanaru C. Systematic reviews of etiology and risk. JBI Manual for Evidence Synthesis. JBI 2020. http://dx.doi.org/10.46658/JBIMES-20-08
[17] Chen S, Liu B, Liu J, Yin N, Wang Y. Comparison of three-dimensional printing and computer-aided engineering in presurgical volumetric assessment of bilateral alveolar clefts. J Craniofac Surg 2020; 31(2): 412-5. http://dx.doi.org/10.1097/SCS.0000000000006011 PMID: 31764559
[18] Du F, Li B, Yin N, Cao Y, Wang Y. Volumetric analysis of alveolar bone defect using three-dimensional-printed models versus computer-aided engineering. J Craniofac Surg 2017; 28(2): 383-6. http://dx.doi.org/10.1097/SCS.0000000000003301 PMID: 28045819
[19] Shirota T, Kurabayashi H, Ogura H, Seki K, Maki K, Shintani S. Analysis of bone volume using computer simulation system for secondary bone graft in alveolar cleft. Int J Oral Maxillofac Surg 2010; 39(9): 904-8. http://dx.doi.org/10.1016/j.ijom.2010.04.050 PMID: 20605410
[20] Abdelhamid M, Marzook HA, Yousef EAS, Tawfik MAM. Evaluation of two computerized methods for presurgical volumetric analysis in secondary alveolar cleft bone grafting: A prospective study. J Contemp Dent Pract 2022; 23(7): 688-94. http://dx.doi.org/10.5005/jp-journals-10024-3366 PMID: 36440514
[21] Chou PY, Denadai R, Hallac RR, *et al*. Comparative volume analysis of alveolar defects by 3D simulation. J Clin Med 2019; 8(9): 1401. http://dx.doi.org/10.3390/jcm8091401 PMID: 31500125
[22] Etemadi Sh M, Movahedian Attar B, Mehdizadeh M, Tajmiri G. Evaluation of the CBCT imaging accuracy in the volumetric assessment of unilateral alveolar cleft. J Stomatol Oral Maxillofac Surg 2021; 122(4): e1-5. http://dx.doi.org/10.1016/j.jormas.2021.06.006 PMID: 34175477
[23] Kasaven CP, McIntyre GT, Mossey PA. Accuracy of both virtual and printed 3-dimensional models for volumetric measurement of alveolar clefts before grafting with alveolar bone compared with a validated algorithm: A preliminary investigation. Br J Oral Maxillofac Surg 2017; 55(1): 31-6. http://dx.doi.org/10.1016/j.bjoms.2016.08.016 PMID: 27608534
[24] Lee D, Atti E, Blackburn J, *et al*. Volumetric assessment of cleft lip and palate defects using cone beam computed tomography. J Calif Dent Assoc 2013; 41(11): 813-7. http://dx.doi.org/10.1080/19424396.2013.12222369 PMID: 24341132
[25] Phienwej K, Chaiworawitkul M, Jotikasthira D, Khwanngern K, Sriwilas P. Comparison of preoperative measurement methods of alveolar cleft volume using cone beam computed tomography between computer simulation and water displacement methods. Cleft Palate Craniofac J 2023; 60(1): 115-21. http://dx.doi.org/10.1177/10556656211055642 PMID: 34841928
[26] Quereshy FA, Barnum G, Demko C, *et al*. Use of cone beam computed tomography to volumetrically assess alveolar cleft defects--preliminary results. J Oral Maxillofac Surg 2012; 70(1): 188-91. http://dx.doi.org/10.1016/j.joms.2011.01.027 PMID: 21549490
[27] Kochhar AS, Sidhu MS, Prabhakar M, *et al*. Intra- And interobserver reliability of bone volume estimation using OsiriX software in patients with cleft lip and palate using cone beam computed tomography. Dent J 2021; 9(2): 14. http://dx.doi.org/10.3390/dj9020014 PMID: 33499043
[28] Chen S, Liu B, Liu J, Yin N, Wang Y. Quick method for presurgical volumetric analysis of alveolar cleft defects. J Craniofac Surg 2020; 31(3): 821-4. http://dx.doi.org/10.1097/SCS.0000000000006235 PMID: 32049901
[29] Chen GC, Sun M, Yin NB, Li HD. A novel method to calculate the volume of alveolar cleft defect before surgery. J Craniofac Surg 2018; 29(2): 342-6. http://dx.doi.org/10.1097/SCS.0000000000004181 PMID: 29239924
[30] Li K, Li S, Liu B, Wang Y. Volumetric analysis of unilateral alveolar bone defect using modified subtraction in older chinese patients. J Craniofac Surg 2023; 34(3): e289-93. http://dx.doi.org/10.1097/SCS.0000000000009209 PMID: 36907840
[31] Liu B, Yin NB, Xiao R, *et al*. Comparison of two methods for presurgical volumetric evaluation of alveolar cleft bone defects

using computer-aided engineering. J Craniofac Surg 2021; 32(2): 477-81.
http://dx.doi.org/10.1097/SCS.0000000000006930 PMID: 33704964

[32] de Rezende Barbosa GL, Wood JS, Pimenta LA, Maria de Almeida S, Tyndall DA. Comparison of different methods to assess alveolar cleft defects in cone beam CT images. Dentomaxillofac Radiol 2016; 45(2): 20150332.
http://dx.doi.org/10.1259/dmfr.20150332 PMID: 26648387

[33] Yu X, Guo R, Li W. Comparison of 2- and 3-dimensional radiologic evaluation of secondary alveolar bone grafting of clefts: A systematic review. Oral Surg Oral Med Oral Pathol Oral Radiol 2020; 130(4): 455-63.
http://dx.doi.org/10.1016/j.oooo.2020.04.815 PMID: 32553577

[34] Kibe T, Maeda-Iino A, Takahashi T, Kamakura S, Suzuki O, Nakamura N. A follow-up study on the clinical outcomes of alveolar reconstruction using octacalcium phosphate granules and atelocollagen complex. J Oral Maxillofac Surg 2021; 79(12): 2462-71.
http://dx.doi.org/10.1016/j.joms.2021.09.017 PMID: 34656516

[35] Makar KG, Buchman SR, Vercler CJ. Bone morphogenetic protein-2 and demineralized bone matrix in difficult bony reconstructions in cleft patients. Plast Reconstr Surg Glob Open 2021; 9(6): 3611.
http://dx.doi.org/10.1097/GOX.0000000000003611 PMID: 34168938

[36] Hung K, Montalvao C, Tanaka R, Kawai T, Bornstein MM. The use and performance of artificial intelligence applications in dental and maxillofacial radiology: A systematic review. Dentomaxillofac Radiol 2020; 49(1): 20190107.
http://dx.doi.org/10.1259/dmfr.20190107 PMID: 31386555

[37] Liang X, Jacobs R, Hassan B, *et al*. A comparative evaluation of Cone Beam Computed Tomography (CBCT) and Multi-Slice CT (MSCT): Part I. On subjective image quality. Eur J Radiol 2010; 75(2): 265-9.
http://dx.doi.org/10.1016/j.ejrad.2009.03.042 PMID: 19410409

[38] Chen H, van Eijnatten M, Aarab G, *et al*. Accuracy of MDCT and CBCT in three-dimensional evaluation of the oropharynx morphology. Eur J Orthod 2018; 40(1): 58-64.
http://dx.doi.org/10.1093/ejo/cjx030 PMID: 28453722

[39] Fokas G, Vaughn VM, Scarfe WC, Bornstein MM. Accuracy of linear measurements on CBCT images related to presurgical implant treatment planning: A systematic review. Clin Oral Implants Res 2018; 29 Suppl 16: 393-415.
http://dx.doi.org/10.1111/clr.13142 PMID: 30328204

[40] Major PW, Johnson DE, Hesse KL, Glover KE. Landmark identification error in posterior anterior cephalometrics. Angle Orthod 1994; 64(6): 447-54.
http://dx.doi.org/10.1043/0003-3219(1994)064<0447:LIEIPA>2.0.CO;2 PMID: 7864466

[41] Ronneberger O, Fischer P, Brox T. U-Net: Convolutional Networks for Biomedical Image Segmentation. In: Navab N, Hornegger J, Wells WM, Eds. Medical Image Computing and Computer-Assisted Intervention – MICCAI 2015. Springer, Cham, 2015, vol. 9351, pp. 234-241.
http://dx.doi.org/10.1007/978-3-319-24574-4_28

[42] Wilson SM, Bautista A, Yen M, Lauderdale S, Eriksson DK. Validity and reliability of four language mapping paradigms. Neuroimage Clin 2017; 16: 399-408.
http://dx.doi.org/10.1016/j.nicl.2016.03.015 PMID: 28879081

[43] Zhang Y, Pei Y, Chen S. Volumetric registration-based cleft volume estimation of alveolar cleft grafting procedures. IEEE 17th International Symposium on Biomedical Imaging (ISBI). Iowa City, IA, USA, 03-07 April 2020, pp. 99-103.
http://dx.doi.org/10.1109/ISBI45749.2020.9098407

[44] Zhang X, Qin N, Zhou Z, Chen S. Machine learning in 3D auto-filling alveolar cleft of CT images to assess the influence of alveolar bone grafting on the development of maxilla. BMC Oral Health 2023; 23(1): 16.
http://dx.doi.org/10.1186/s12903-023-02706-8 PMID: 36631872

[45] Wu P, Hu L, Li H, *et al*. Clinical application and accuracy analysis of 3D printing guide plate based on polylactic acid in mandible reconstruction with fibula flap. Ann Transl Med 2021; 9(6): 460-0.
http://dx.doi.org/10.21037/atm-20-6781 PMID: 33850857

[46] Etemad-Shahidi Y, Qallandar OB, Evenden J, Alifui-Segbaya F, Ahmed KE. Accuracy of 3-dimensionally printed full-arch dental models: A systematic review. J Clin Med 2020; 9(10): 3357.
http://dx.doi.org/10.3390/jcm9103357 PMID: 33092047

[47] Shen J, Fisher DM, Yasabala B, Wong Riff KWY, Podolsky DJ. The first alveolar bone graft simulator. Plast Reconstr Surg Glob Open 2023; 11(10): 5363.
http://dx.doi.org/10.1097/GOX.0000000000005363 PMID: 37908329

[48] Rendón-Medina MA, Arias-Salazar L, Covarrubias-Noriega A, *et al*. 3D printing for surgical planning in bone grafts for cleft-palate: A case report. Int J Res Med Sci 2023; 11(2): 688-90.
http://dx.doi.org/10.18203/2320-6012.ijrms20230186

[49] Ahn G, Lee JS, Yun WS, Shim JH, Lee UL. Cleft alveolus reconstruction using a three-dimensional printed bioresorbable scaffold with human bone marrow cells. J Craniofac Surg 2018; 29(7): 1880-3.
http://dx.doi.org/10.1097/SCS.0000000000004747 PMID: 30028404

[50] Leal CR, de Carvalho RM, Ozawa TO, *et al*. Outcomes of Alveolar Graft With Rhbmp-2 in CLP: Influence of Cleft Type and Width, Canine Eruption, and Surgeon. Cleft Palate Craniofac J 2019; 56(3): 383-9.
http://dx.doi.org/10.1177/1055665618780981 PMID: 29924638

[51] Sakamoto Y, Ogata H, Miyamoto J, Kishi K. The role of surgeon's learning on the outcomes of alveolar bone graft for cleft repair. J Plast Reconstr Aesthet Surg 2022; 75(6): 1937-41.
http://dx.doi.org/10.1016/j.bjps.2021.11.114 PMID: 34969628

[52] Enemark H, Sindet-Pedersen S, Bundgaard M. Long-term results after secondary bone grafting of alveolar clefts. J Oral Maxillofac Surg 1987; 45(11): 913-8.
http://dx.doi.org/10.1016/0278-2391(87)90439-3 PMID: 3312537

[53] Bergland O, Semb G, Abyholm FE. Elimination of the residual alveolar cleft by secondary bone grafting and subsequent orthodontic treatment. Cleft Palate J 1986; 23(3): 175-205.
PMID: 3524905

[54] Kindelan JD, Nashed RR, Bromige MR. Radiographic assessment of secondary autogenous alveolar bone grafting in cleft lip and palate patients. Cleft Palate Craniofac J 1997; 34(3): 195-8.
http://dx.doi.org/10.1597/1545-1569_1997_034_0195_raosaa_2.3.co_2 PMID: 9167068

[55] Witherow H, Cox S, Jones E, Carr R, Waterhouse N. A new scale to assess radiographic success of secondary alveolar bone grafts. Cleft Palate Craniofac J 2002; 39(3): 255-60.
http://dx.doi.org/10.1597/1545-1569_2002_039_0255_anstar_2.0.co_2 PMID: 12019000

[56] Khalil W, de Musis CR, Volpato LER, Veiga KA, Vieira EMM, Aranha AM. Clinical and radiographic assessment of secondary bone graft outcomes in cleft lip and palate patients. Int Sch Res Notices 2014; 2014: 1-8.
http://dx.doi.org/10.1155/2014/231795 PMID: 27351004

[57] Yu X, Huang Y, Li W. Correlation between alveolar cleft morphology and the outcome of secondary alveolar bone grafting for unilateral cleft lip and palate. BMC Oral Health 2022; 22(1): 251.
http://dx.doi.org/10.1186/s12903-022-02265-4 PMID: 35733126

[58] Sander M, Daskalogiannakis J, Tompson B, Forrest C. Effect of alveolar bone grafting on nasal morphology, symmetry, and nostril shape of patients with unilateral cleft lip and palate. Cleft Palate Craniofac J 2011; 48(1): 20-7.
http://dx.doi.org/10.1597/09-007 PMID: 20170388

[59] Chu YY, Chang FCS, Lu TC, Lee CH, Chen PKT. Surgical outcomes of secondary alveolar bone grafting and extensive gingivoperiosteoplasty performed at mixed dentition stage in unilateral complete cleft lip and palate. J Clin Med 2020; 9(2): 576.

http://dx.doi.org/10.3390/jcm9020576 PMID: 32093231

[60] Hynes PJ, Earley MJ. Assessment of secondary alveolar bone grafting using a modification of the Bergland grading system. Br J Plast Surg 2003; 56(7): 630-6. http://dx.doi.org/10.1016/S0007-1226(03)00361-8 PMID: 12969660

[61] Murali SP, Denadai R, Chou PY, Chang CS, Lo LJ. Secondary alveolar bone grafting in patients with cleft lip and palate: A step-by-step video series. Plast Reconstr Surg 2022; 149(6): 1176e-80e. http://dx.doi.org/10.1097/PRS.0000000000009168 PMID: 35413047

[62] Nagashima H, Sakamoto Y, Ogata H, Miyamoto J, Yazawa M, Kishi K. Evaluation of bone volume after secondary bone grafting in unilateral alveolar cleft using computer-aided engineering. Cleft Palate Craniofac J 2014; 51(6): 665-8. http://dx.doi.org/10.1597/13-045 PMID: 24004421

[63] Al-Ekrish AA, Ekram M. A comparative study of the accuracy and reliability of multidetector computed tomography and cone beam computed tomography in the assessment of dental implant site dimensions. Dentomaxillofac Radiol 2011; 40(2): 67-75. http://dx.doi.org/10.1259/dmfr/27546065 PMID: 21239568